

Rhodanine side-chained thiophene and indacenodithiophene copolymer for solar cell applications

Meijie Fan ^{a, b}, Linrui Duan ^b, Yuanhang Zhou ^b, Shuguang Wen ^b, Feng Li ^c, Deyu Liu ^b, Mingliang Sun ^{a, *}, Renqiang Yang ^b

^a Institute of Materials Science and Engineering, Ocean University of China, Qingdao 266100, China

^b CAS Key Laboratory of Bio-Based Materials, Qingdao Institute of Bioenergy and Bioprocess Technology, Chinese Academy of Sciences, Qingdao 266101, China

^c Key Laboratory of Rubber-Plastics of Ministry of Education/Shandong Province, School of Polymer Science and Engineering, Qingdao University of Science & Technology, 53 Zhengzhou Road, Qingdao 266042, China

ARTICLE INFO

Article history:

Received 14 April 2017

Received in revised form

10 June 2017

Accepted 9 July 2017

Available online 19 July 2017

Keywords:

Polymer solar cells

Side chain

Indacenodithiophene

Rhodanine

ABSTRACT

In this work, 2-(3-ethyl-4-oxothiazolidin-2-ylidene)malononitrile is connected on the β position of thiophene, and this monomer is copolymerized with indacenodithiophene (IDT) to build one novel photovoltaic polymer (PIDTPCR). The highest occupied molecular orbital (HOMO) and the lowest unoccupied molecular orbital (LUMO) level of the polymer is -5.26 eV and -3.45 eV, respectively. Compared with reference polymer without rhodanine side chain, PIDTPCR polymer shows low band gap and low energy level which contribute to the J_{sc} and V_{oc} of the PSCs devices. The best performance parameters of the solar cells devices are V_{oc} (0.91 V), J_{sc} (10.1 mA/cm²), FF (52.4%) and PCE (5.18%).

© 2017 Elsevier Ltd. All rights reserved.

1. Introduction

Polymer solar cells (PSCs) have drawn a great deal of attention due to their unique features for low cost, easy processing, low weight, flexibility, and large-area fabrication [1–5]. It is an efficient strategy using donor–acceptor (D–A) copolymer to optimize the photovoltaic polymers properties [6,7], because D–A copolymer can form an intramolecular charge transfer (ICT) state which widens the polymer light absorption. The strength of ICT state varies with different donor and acceptor units, so the changes of donor and acceptor units can optimize polymers photovoltaic performances [8]. Through donor and acceptor design, the polymer optical band gap match well with solar spectrum and the energy levels match with that of PCBM, and then the PSCs devices performance can be improved [9]. Therefore, appropriate donor and acceptor units play a very essential role in D–A polymer design. On this basis, many

novel donor–acceptor (D–A) conjugated copolymers have been widely developed and applied to PSCs with PCE over 12% [10–14].

Indacenodithiophene (IDT) with highly planar structure has been demonstrated as a promising build block for polymer donor materials because of its extraordinary electron-donating and hole transporting performance [15,16]. IDT based conjugated polymers were widely applied in PSCs and showed broad absorption and high molar extinction coefficient, which is beneficial to obtaining high short circuit current (J_{sc}) [17,18]. The solubility of IDT polymer can be easily increased by attaching functional side chains due to the effect of sp^3 -hybridized carbon atoms on the IDT [16,19,20]. Rhodanine, as an electron withdrawing unit, can effectively induce intramolecular charge transfer and improve optical absorption properties. Rhodanine is widely used as end capping group in photovoltaic small molecule, while there is very few report about rhodanine used in photovoltaic polymer [21–23]. As an alternative method to design D–A polymer with donor and acceptor unit both in polymer backbone, electron deficient side chains introduced to polymer backbone can also effectively broaden absorption spectrum and deepen energy levels [24]. This method has been proved to be successful in many polymer systems [25–28].

* Corresponding author.

E-mail addresses: mlsun@ouc.edu.cn (M. Sun), yangrq@qibebt.ac.cn (R. Yang).

In this work, we have synthesized a polymer based on IDT and 2-(5-((2,5-dibromothiophene-3-yl)methylene)-3-ethyl-4-oxothiazolidin-2-ylidene)malononitrile units to investigate the influence of rhodanine side chain on the thiophene and IDT backbone polymer. We have compared our test results with the polymer based IDT and thiophene in literature without rhodanine side chain [29]. The introduction of rhodanine side chain can widen absorption spectrum; and the highest occupied molecular orbital energy level (HOMO) and the lowest unoccupied molecular orbital energy level (LUMO) of the resulted polymer have been deepened. As a result of the deep energy levels, the best open circuit voltage (V_{oc}) of PSCs devices is 0.91 V and the PCE has also been improved accordingly.

2. Experimental

All of the reagents were purchased from commercial sources. They did not need further purification before used, unless otherwise noted. Toluene and diethyl ether were dried by sodium, and benzophenone was used as indicator. N,N-dimethylformamine (DMF) was distilled with calcium hydride. 2-(3-Ethyl-4-oxothiazolidin-2-ylidene)malononitrile was synthesized in our laboratory. Indacenodithiophene was purchased from Derthon optoelectronic materials science technology co. LTD.

2.1. Instruments

NMR spectra were measured on a Bruker Advance III60 Spectrometer. Gel permeation chromatography (GPC) on a HLC-8320 instrument was used to obtain the molecular weights of the polymer; tetrahydrofuran (THF) was used as eluent; polystyrenes were used as reference. The Ultraviolet–visible (UV–vis) absorption spectra were recorded on a Lambda 25 spectrophotometer. The thermogravimetric analysis (TGA) was characterized with SDT-Q600 instrument under nitrogen atmosphere. Cyclic voltammetry (CV) was estimated by a CHI660D electrochemical workstation. Three-electrode system consists of glassy carbon working electrode, Pt wire counter electrode and saturated calomel reference electrode. The test was performed under tetrabutylammonium phosphorus hexafluoride (Bu_4NPF_6 , 0.1 M) in acetonitrile solution as the supporting electrolyte, with the scan rate of 100 mV/s and ferrocene/ferrocenium (Fc/Fc^+) as the internal standard. AFM studies were conducted on an Agilent 5400 instrument. X-ray diffraction (XRD) pattern was determined with a Bruker D8 Advance.

2.2. Device fabrication

Photovoltaic devices were fabricated in the structure of ITO/PEDOT:PSS (30 nm)/polymer:PCBM/PFN/Al (100 nm). ITO coated glass substrates are cleaned with ITO lotion, distilled water, acetone and isopropyl alcohol sequentially. Then the ITO coated glass substrates were treated by oxygen plasma. PEDOT:PSS were spin-coated on the ITO substrates. Then polymer and PC₇₁BM were blended in o-dichlorobenzene in the ratio of 1:1, 1:2, 1:3 and 1:4. The prepared solutions were stirred overnight in glove box. The polymer and PC₇₁BM blends were spin-coated on the ITO/PEDOT:PSS substrates. Then PFN was spin-coated on the top of the active layer from absolute methanol solution with concentration around 0.2 mg/mL, and the final PFN thickness was around 5 nm. Finally, Al was thermally evaporated on the top of PFN. Photovoltaic performances were obtained under the illumination of AM 1.5G

(100 mWcm⁻²) in nitrogen atmosphere. J–V data were collected by a Keithley 2420 source meter.

2.3. Synthesis

2.3.1. Thiophene-3-carbaldehyde

A solution of 3-bromothiophene (10 g, 61.3 mmol) in 60 mL of dried diethyl ether was cooled to -78°C , and then 27 mL of n-butyl lithium (2.5 M in hexane, 67.5 mmol) was added dropwise. The reaction mixture was stirred for 1 h. Subsequently, a solution of N,N-dimethylformamine (DMF, 6.72 g, 92 mmol) in 20 mL of diethyl ether was added dropwise. The reaction mixture was kept at -78°C for additional 30 min and then the mixture was warmed to room temperature. The reaction was stirred for 45 min at ambient temperature and then quenched by water. The mixture was extracted with diethyl ether. The organic phase was dried over anhydrous sodium sulfate and concentrated via rotary evaporation. The residue was purified by silica gel chromatography with an eluent of dichloromethane/hexanes (1/2) to obtain a product (5.59 g, 81.3%) as a yellow oil. ¹H NMR (600 MHz, CDCl₃) δ (ppm) 9.93 (s, 1H), 8.13 (d, 1H), 7.54 (d, 1H), 7.38 (dd, 1H).

2.3.2. 2,5-Dibromothiophene-3-carbaldehyde [30]

A solution of thiophene-3-carboxaldehyde (3.6 g, 32.1 mmol) in 30 mL of dried N,N-dimethylformamine (DMF) was stirred at room temperature in dark. A solution of N-bromosuccinimide (NBS) (17.14 g, 96.3 mmol) in 33 mL of DMF was added dropwise. The mixture was stirred for 48 h. The reaction was finished, and the solution was quenched with water and extracted several times with diethyl ether. The organic phases were collected and dried with anhydrous Na₂SO₄. After evaporation, the concentrated part was purified by column chromatography with an eluent of dichloromethane/hexanes (1/1). After removal of solvent, the product was recrystallized from n-hexane. A yellow crystalline solid was obtained. ¹H NMR (600 MHz, CDCl₃) δ (ppm) 9.80 (s, 1H), 7.34 (s, 1H).

2.3.3. 2-(5-((2,5-Dibromothiophen-3-yl)methylene)-3-ethyl-4-oxothiazolidin-2-ylidene)malononitrile [31]

A mixture of 2,5-dibromothiophene-3-carbaldehyde (500 mg, 1.85 mmol), 2-(3-ethyl-4-oxothiazolidin-2-ylidene)malononitrile (715.8 mg, 3.7 mmol), and basic aluminum oxide (1.03 g) reacted in dry toluene (50 mL) at 70°C for 3 h and cooled to ambient temperature. The filtrate was collected by filtration and the residue thoroughly was washed with toluene. The solvent of the filtrate was removed by evaporation, and the crude product was purified by column chromatography on silica with CH₂Cl₂ to give a green yellow solid (499 mg, 60%). ¹H NMR (600 MHz, CDCl₃) δ (ppm) 7.83 (s, 1H), 7.26 (s, 1H), 4.33 (q, 2H), 1.42 (t, 3H). ¹³C NMR (151 MHz, CDCl₃) δ (ppm) 165.90, 164.80, 134.45, 127.61, 126.99, 121.78, 117.94, 114.59, 112.81, 111.76, 56.79, 40.88, 14.16. HRMS (EI) calcd for C₁₃H₇Br₂N₃O₂ [M+H]⁺: 445.15, found: 445.00.

2.3.4. Synthesis of PIDTPCR

Indacenodithiophene-Sn (184.95 mg, 0.15 mmol), 2-(5-((2,5-dibromothiophene-3-yl)methylene)-3-ethyl-4-oxothiazolidin-2-ylidene)malononitrile (66.77 mg, 0.15 mmol), Pd₂(dba)₃ (4.12 mg, 0.0045 mmol), and tri(o-tolyl)phosphine (8.24 mg, 0.027 mmol) were added in a 25 mL flask. The system was purged with nitrogen for three times. After the addition of toluene (5 mL), the mixture was heated to 115°C and maintained for 48 h under nitrogen protection. After cooling to ambient temperature, the mixture was precipitated into methanol and collected by filtration. The polymer was dealt with a Soxhlet funnel and extracted by acetone, hexane and chloroform,

successively. The part of chloroformic solution was collected and dried. The polymer PIDTPCR was obtained (170 mg, 67%). ^1H NMR (600 MHz, CDCl_3) δ 7.50–7.41 (m, 2H), 7.20–7.05 (m, 20H), 4.34 (dr, 2H), 2.57 (dr, 8H), 1.59–0.87 (m, 47H). Elemental analysis calcd (%) for $[\text{C}_{79}\text{H}_{85}\text{N}_3\text{OS}_4]$: C 77.72%, H 7.02%, N 3.44%; found: C 76.84%, H 6.79%, N 3.46%.

3. Results and discussion

3.1. Synthesis and characterization

The polymer PIDTPCR was synthesized by stille coupling reactions as shown in Scheme 1. The side chains on the IDT ensure that PIDTPCR was readily dissolved in chloroform, chlorobenzene and o-dichlorobenzene. The number-average molecular (M_n) of PIDTPCR is 12 KDa with a polydispersity index (PDI) of 1.32 measured by gel permeation chromatography (GPC). Thermal gravity analysis (TGA) measurement demonstrated that the decomposition temperature (T_d) of the polymer is 389.1 °C. The polymer possesses good thermal stability. The TGA curve is exhibited in Fig. 1.

3.2. UV–vis absorption and electrochemical properties

The UV–visible absorption spectra of PIDTPCR in diluted chloroform solution and in thin film were exhibited in Fig. 2. The short wavelength absorption of the polymer was showed at around 365 nm corresponding to the delocalized excitonic π – π^* transitions [32]. The long wavelength absorption of the polymer was presented at around 450 nm–650 nm originated from intra-molecular charge transfer (ICT) between the acceptor and donor units [33]. Compared with the UV–visible absorption spectra in solution, the absorption peak of the film is broad due to the intensive intermolecular interactions [34]. Based on the absorption onsets of the thin films, the optical band gap (E_g^{opt}) is calculated to be 1.81 eV. Compared with the previous reported polymer without rhodanine side chain [29], the absorption onset is extended from 590 nm to 685 nm in the film. There are two possible reasons lead to this result. One is the vinylene linkage of PIDTPCR polymer promotes the coplanarity and increases conjugation [25]. The other is the intramolecular charge transfer (ICT) between the

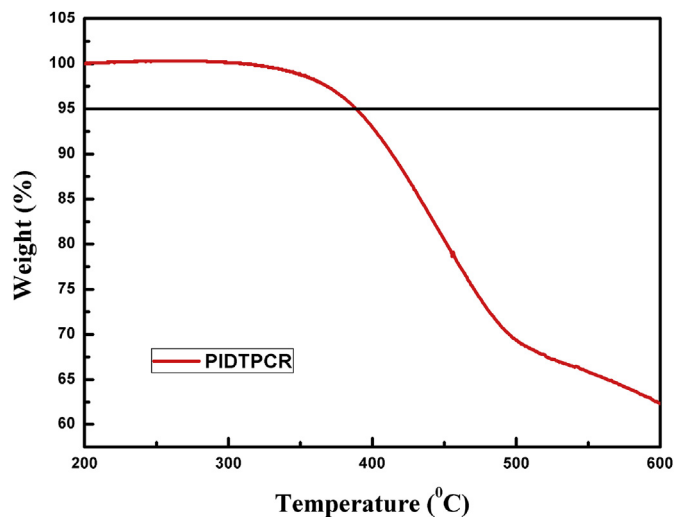


Fig. 1. TGA of PIDTPCR polymer.

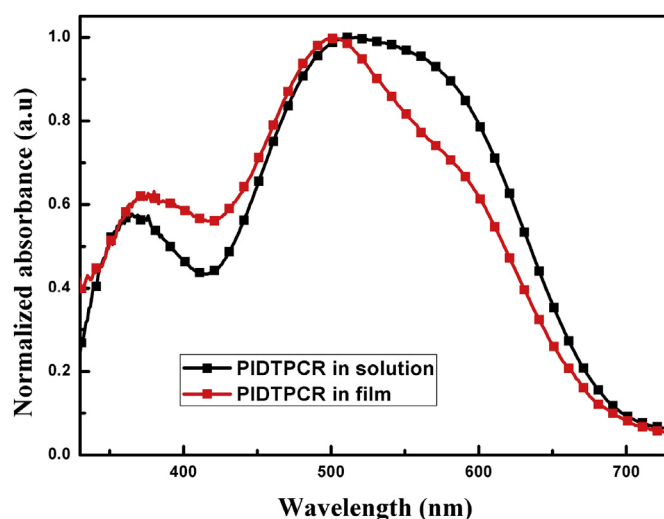
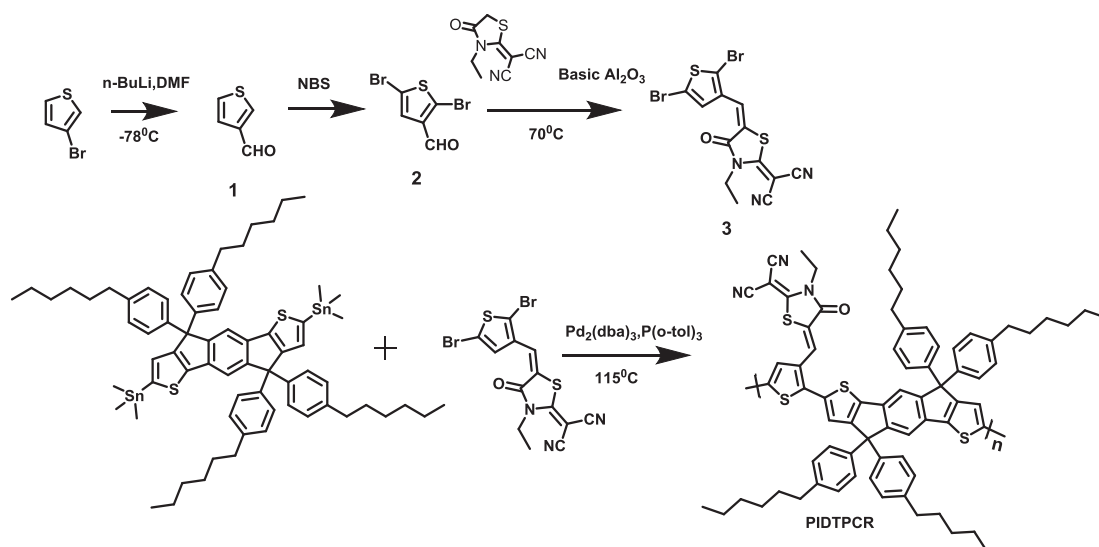


Fig. 2. UV–vis absorption spectra of PIDTPCR in chloroform solution and in thin film.



Scheme 1. Synthetic routes for the polymer.

Table 1
Molecular weights, optical and electrochemical properties of PIDTPCR and reference polymer.

Polymer	M_w (PDI)	λ_{max} (nm)	E_g^{opt} (eV)	HOMO (eV)	LUMO (eV)	Ref
P3	48,700 (2.19)	510	2.08	−5.1	−3.02	[29]
PIDTPCR	16,700 (1.32)	511	1.81	−5.26	−3.45	

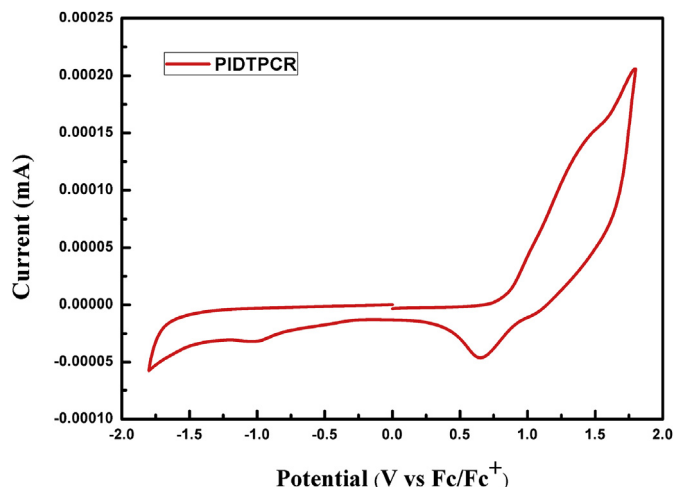


Fig. 3. Cyclic voltammogram of the polymer film.

electron-accepting side chain and electron-donating main chain [26]. And the related data were listed in Table 1.

The electrochemical property of PIDTPCR was demonstrated by the electrochemical cyclic voltammetry (CV). The CV curve was

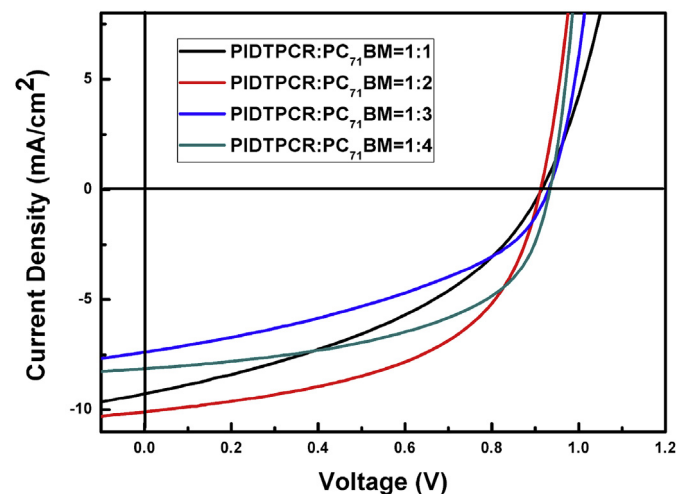


Fig. 4. J–V curves of PSCs devices under the illumination of AM 1.5G, 100 mWcm^{−2}.

Table 2
PSCs devices performances.

Polymer	Polymer:PC ₇₁ BM	J_{sc} (mA/cm ²)	V_{oc} (V)	FF	PCE (%)	Ref
P3	1:3	7.6	0.80	0.54	3.3	[29]
PIDTPCR	1:1	9.26 (8.85)	0.91 (0.93)	0.40 (0.38)	3.67 (3.39)	This work
PIDTPCR	1:2	10.1 (9.72)	0.91 (0.92)	0.52 (0.51)	5.18 (4.89)	This work
PIDTPCR	1:3	7.07 (7.22)	0.94 (0.93)	0.44 (0.43)	3.15 (3.09)	This work
PIDTPCR	1:4	8.12 (8.08)	0.93 (0.92)	0.54 (0.53)	4.38 (4.23)	This work

Values in parentheses are average data from 6 devices.

shown in Fig. 3. And the onset oxidation potential (E_{ox}) is 0.85 V. The HOMO was −5.26 eV obtained by the equations: $HOMO = -(E_{ox} + 4.41)$ (eV), according to the energy level of the Fc/Fc^+ versus saturated calomel electrode (SCE). The LUMO was −3.45 eV estimated by the HOMO level and optical band gap. The energy level of PIDTPCR is deeper than the polymer based on IDT and thiophene without rhodanine side chain, and these results were compared in Table 1 [29]. The deep HOMO energy level of the polymer will lead to higher PSCs V_{oc} .

3.3. Photovoltaic performance

To characterize photovoltaic properties of PIDTPCR, PSCs devices were prepared in a configuration of ITO/PEDOT:PSS(30 nm)/polymer:PC₇₁BM(120 nm)/PFN(5 nm)/Al(100 nm). To obtain the optimized devices, the PIDTPCR:PC₇₁BM blend ratios were adjusted from 1:1 to 1:4, and the concentration of blends in o-dichlorobenzene is 30 mg/mL. The best performance parameters of the devices are V_{oc} (0.91 V), J_{sc} (10.1 mA/cm²), FF (52.4%) and PCE (5.18%) with a PIDTPCR:PC₇₁BM weight ratio of 1:2. The J–V curves of PSCs devices with the different weight ratios were shown in Fig. 4. We have compared the optimal performances of the polymer with other report about the polymer based on IDT and thiophene units without rhodanine side chain [29]. And the comparison data were listed below as Table 2. To highlight the high V_{oc} , the donor photon energy loss defined as $E_g - eV_{oc}$ was introduced [35], where E_g is the optical band gap of the polymer. The value of $E_g - eV_{oc}$ for PIDTPCR is 0.9 eV, while the value of $E_g - eV_{oc}$ for P3 is 1.28 eV. The PIDTPCR based devices show lower energy loss, so the introduction of the rhodanine side chain can improve the photovoltaic performance. The external quantum efficiency (EQE) curve has been measured to verify the accuracy of the device performances under the optimal conditions and shown in Fig. 5. The PSCs device absorbs sunlight from 319 nm to 700 nm, and the maximum incident photon to current efficiency appears at 439 nm. The J_{sc} calculated from EQE matched with the J_{sc} measured by J–V curve (within 5% error). Compared with P3, the device of PIDTPCR has a broader photo response range and the maximum IPCE show improvement. These contribute to the larger J_{sc} . Hole mobility was characterized by the space-charge-limited current (SCLC) method. The device structure is ITO/PEDOT:PSS/PIDTPCR:PC₇₁BM/Ag. The test result calculated by Mott–Gurney equation was $7.0 \times 10^{-4} \text{ cm}^2 \text{ V}^{-1} \text{ s}^{-1}$. The FF of PIDTPCR based PSCs devices (Table 2) was slightly lower than P3 (reference polymer), and the relative low hole mobility of PIDTPCR may be one possible reason. The SCLC curve was plotted in Fig. 6.

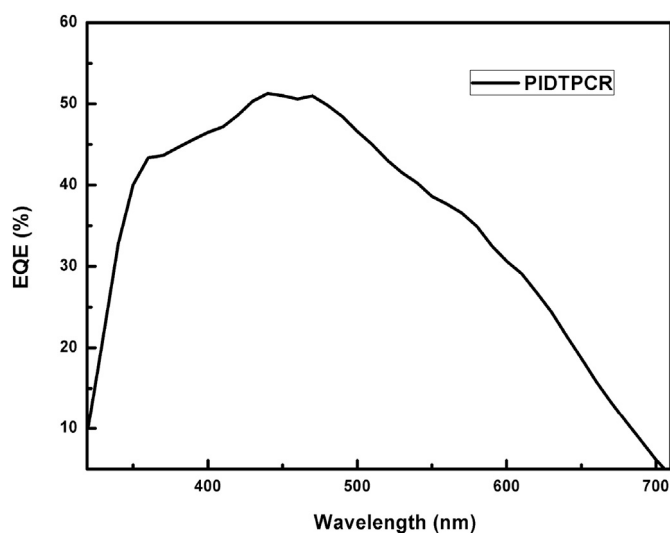


Fig. 5. EQE curve of the best PCE device.

3.4. Morphological properties

The topography of active layer is a crucial factor for PSCs device properties. Atomic force microscope (AFM) was used to explore the active layer's morphology and the surface topography was

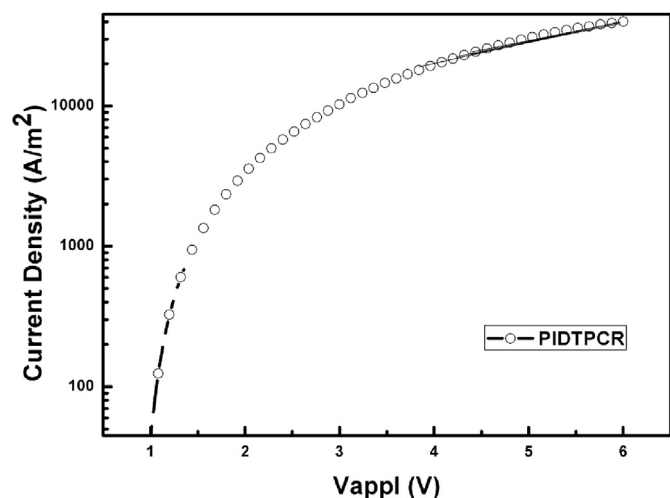


Fig. 6. SCLC characteristics of PIDTPCR.

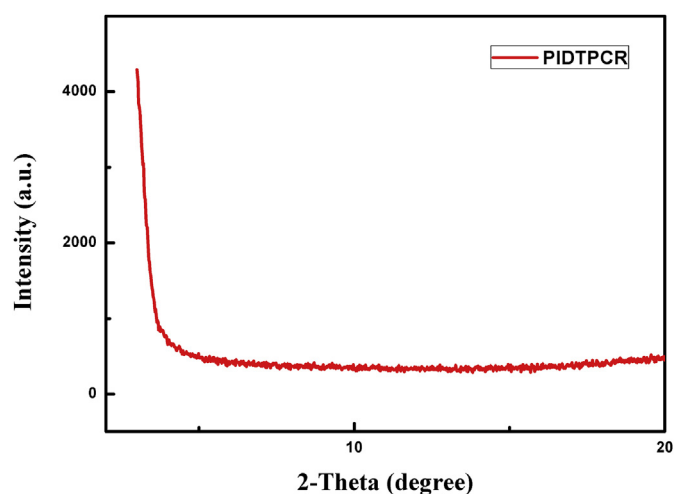


Fig. 8. XRD pattern of the polymer thin film.

exhibited in Fig. 7. The root-mean-square roughness was around 1 nm. The active layer has formed good interpenetrating network structure and appropriate phase separation [36]. This structure contributes to the improvement of J_{SC} and FF, so that the PCE can be enhanced. In order to analysis the crystallinity of the polymer, X-ray diffraction (XRD) test were carried out. From Fig. 8, we can conclude that the polymer is amorphous.

4. Conclusion

In summary, we have successfully introduced 2-(3-ethyl-4-oxothiazolidin-2-ylidene) malononitrile to the β position of thiophene to build one new monomer for IDT polymer. Compared with the polymer without rhodanine side-chain, the UV–vis absorption and EQE photo response of the new polymer have been broadened. The energy levels were deepened. The PSCs PCE was improved to 5.18% with V_{oc} (0.91 V), J_{sc} (10.1 mA/cm²) and FF (52.4%). The novel monomer is a promising unit in polymer solar cell donor materials design.

Acknowledgements

The authors gratefully acknowledge financial support from the NSFC (51573205 and 21274134).

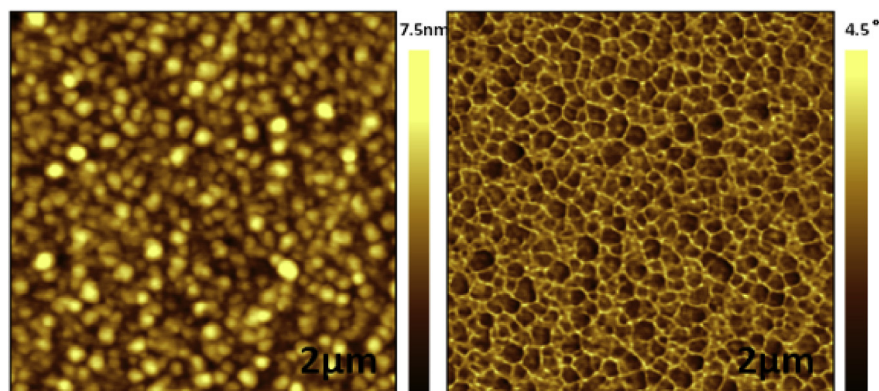


Fig. 7. AFM image of PSCs active layer (topography and phase) (2x2 μ m).

References

- [1] J.G.G. Yu, J.C. Hummelen, F. Wudl, A.J. Heeger, *Science* 270 (1995) 1789–1791.
- [2] S. Gunes, H. Neugebauer, N.S. Sariciftci, *Chem. Rev.* 107 (2007) 1324–1338.
- [3] E. Zhou, S. Yamakawa, K. Tajima, C. Yang, K. Hashimoto, *Chem. Mater.* 21 (2009) 4055–4061.
- [4] Z. He, C. Zhong, X. Huang, W.Y. Wong, H. Wu, L. Chen, S. Su, Y. Cao, *Adv. Mater.* 23 (2011) 4636–4643.
- [5] M. Fan, Z. Du, W. Chen, D. Liu, S. Wen, M. Sun, R. Yang, *Asian J. Org. Chem.* 5 (2016) 1273–1279.
- [6] D. Liu, C. Gu, M. Xiao, M. Qiu, M. Sun, R. Yang, *Polym. Chem.* 6 (2015) 3398–3406.
- [7] P. Peumans, A. Yakimov, S.R. Forrest, *J. Appl. Phys.* 93 (2003) 3693–3723.
- [8] Y.J. Cheng, S.H. Yang, C.S. Hsu, *Chem. Rev.* 109 (2009) 5868–5923.
- [9] J.W. Lee, H. Ahn, W.H. Jo, *Macromolecules* 48 (2015) 7836–7842.
- [10] Z.C. He, C.M. Zhong, S.J. Su, M. Xu, H.B. Wu, Y. Cao, *Nat. Photonics* 6 (2012) 591–595.
- [11] J.D. Chen, C. Cui, Y.Q. Li, L. Zhou, Q.D. Ou, C. Li, Y. Li, J.X. Tang, *Adv. Mater.* 27 (2015) 1035–1041.
- [12] D. Ding, W. Chen, J. Wang, M. Qiu, H. Zheng, J. Ren, M. Fan, M. Sun, R. Yang, *J. Mater. Chem. C* 4 (2016) 8716–8723.
- [13] W. Zhao, D. Qian, S. Zhang, S. Li, O. Inganas, F. Gao, J. Hou, *Adv. Mater.* 28 (2016) 4734–4739.
- [14] W.R. Mateker, M.D. McGehee, *Adv. Mater.* (2016) 1603940.
- [15] M. Zhang, X. Guo, X. Wang, H. Wang, Y. Li, *Chem. Mater.* 23 (2011) 4264–4270.
- [16] C.M. Cho, Q. Ye, W.T. Neo, T. Lin, J. Song, X. Lu, J. Xu, *J. Mater. Sci.* 50 (2015) 5856–5864.
- [17] W. Zhang, J. Smith, S.E. Watkins, R. Gysel, M. McGehee, A. Salleo, J. Kirkpatrick, S. Ashraf, T. Anthopoulos, M. Heeney, I. McCulloch, *J. Am. Chem. Soc.* 132 (2010) 11437–11439.
- [18] D. Liu, L. Sun, Z. Du, M. Xiao, C. Gu, T. Wang, S. Wen, M. Sun, R. Yang, *RSC Adv.* 4 (2014) 37934.
- [19] X. Liu, Q. Li, Y. Li, X. Gong, S. Su, Y. Cao, *J. Mater. Chem. A* 2 (2014) 4004–4013.
- [20] D. Dang, W. Chen, S. Himmelberger, Q. Tao, A. Lundin, R. Yang, W. Zhu, A. Salleo, C. Müller, E. Wang, *Adv. Energy Mater.* 4 (2014) 1400680.
- [21] H. Bai, Y. Wang, P. Cheng, Y. Li, D. Zhu, X. Zhan, *ACS Appl. Mater. Interfaces* 6 (2014) 8426–8433.
- [22] Y. Liu, X. Wan, F. Wang, J. Zhou, G. Long, J. Tian, Y. Chen, *Adv. Mater.* 23 (2011) 5387–5391.
- [23] J. Zhou, X. Wan, Y. Liu, Y. Zuo, Z. Li, G. He, G. Long, W. Ni, C. Li, X. Su, Y. Chen, *J. Am. Chem. Soc.* 134 (2012) 16345–16351.
- [24] F. Huang, K.S. Chen, H.L. Yip, S.K. Hau, O. Acton, Y. Zhang, J. Luo, A.K. Jen, *J. Am. Chem. Soc.* 131 (2009) 13886–13887.
- [25] Z. Gu, P. Tang, B. Zhao, H. Luo, X. Guo, H. Chen, G. Yu, X. Liu, P. Shen, S. Tan, *Macromolecules* 45 (2012) 2359–2366.
- [26] H. Tan, X. Deng, J. Yu, B. Zhao, Y. Wang, Y. Liu, W. Zhu, H. Wu, Y. Cao, *Macromolecules* 46 (2013) 113–118.
- [27] P. Shen, H. Bin, L. Xiao, Y. Li, *Macromolecules* 46 (2013) 9575–9586.
- [28] E. Zhu, J. Hai, Z. Wang, B. Ni, Y. Jiang, L. Bian, F. Zhang, W. Tang, *J. Phys. Chem. C* 117 (2013) 24700–24709.
- [29] S.-H. Chan, C.-P. Chen, T.-C. Chao, C. Ting, C.-S. Lin, B.-T. Ko, *Macromolecules* 41 (2008) 5519–5526.
- [30] C.G. Maria, T. Francesca, P. Daniela, B. Chiara, F. Alessandra, Z. Gianni, *Macromol. Chem. Phys.* 202 (10) (2001).
- [31] L.Y. Lin, Y.H. Chen, Z.Y. Huang, H.W. Lin, S.H. Chou, F. Lin, C.W. Chen, Y.H. Liu, K.T. Wong, *J. Am. Chem. Soc.* 133 (2011) 15822–15825.
- [32] J.-M. Jiang, H.-K. Lin, Y.-C. Lin, H.-C. Chen, S.-C. Lan, C.-K. Chang, K.-H. Wei, *Macromolecules* 47 (2014) 70–78.
- [33] C.-P. Chen, Y.-C. Chen, C.-Y. Yu, *Polym. Chem.* 4 (2013) 1161–1166.
- [34] N. Wang, Z. Chen, W. Wei, Z. Jiang, *J. Am. Chem. Soc.* 135 (2013) 17060–17068.
- [35] M. Wang, H. Wang, T. Yokoyama, X. Liu, Y. Huang, Y. Zhang, T.Q. Nguyen, S. Aramaki, G.C. Bazan, *J. Am. Chem. Soc.* 136 (2014) 12576–12579.
- [36] B. Liu, X. Chen, Y. Zou, Y. He, L. Xiao, X. Xu, L. Li, Y. Li, *Polym. Chem.* 4 (2013) 470–476.